A MAC and PHY Cross-Layer Model to Estimate the Cell Coverage of IEEE 802.11a, 802.11b and 802.11g WLANs

Roger Pierre Fabris Hoefel

Electrical Engineering Department - Federal University of Rio Grande do Sul (UFRGS)
Av. Osvaldo Aranha, 103 - CEP: 90035-190 – Porto Alegre – RS – Brazil

roger.hoefel@ufrgs.br

Abstract. *It is proposed and validated a theoretical medium access control (MAC) and physical (PHY) cross-layer model to calculate the link budget and to estimate the cell coverage of IEEE 802.11a, 802.11b and 802.11g wireless local area networks (WLANs). The applied methodology takes into account jointly the goodput, the traffic load, the channel modelling, the receiver structures and the link analyses.*

Resumo. *Neste artigo é proposto e validado um modelo teórico que analisa de maneira integrada o desempenho das camadas de enlace e física com o objetivo de estimar a cobertura das redes locais sem fio IEEE 802.11a, 802.11b e 802.11g. As expressões analíticas propostas permitem relacionar a eficiência e a coberturas das redes locais com os protocolos de enlace (e.g. algoritmo de resolução da janela de contenção), com os protocolos da camada física (e.g. esquemas de modulação, correção de erros), com os modelos do canal de rádio móvel e com a carga de tráfico no sistema.*

1. Introduction and Related Work

The estimation of the cell coverage is a fundamental issue to a cost effective deployment of IEEE 802.11 WLANs. Therefore, researchers from academy, developers of equipments and broadband wireless integrators have published peer-review papers, application notes, white papers and software tools in order to systematize and optimize the cell planning procedures. In [Intersil 1998] is presented a basic link budget for IEEE 802.11b networks, where the link budget is defined as the calculations and tabulations of the useful signal power and the interference power at the receiver input. The Wireless Connections (http://www.wirelessconnections.net) and Terabean (http://www.terabeam.com), integrators of wireless broadband solutions, have provided basic software tools to estimate the link budget. Researchers from AT&T Labs have presented in [Clark 2002] a basic link analyzes for IEEE 802.11 outdoor cellular networks. In [Kappes 2004] algorithms are developed to estimate access points (APs) placements and cell coverage based on signal strength estimations. Our Brazilian Research Community has also been developing research activities directly related with the field of our contribution: *(1) Ramela* and *de Rezende* [Ramela 2006] proposed an analytical model to estimate the reduction of interference, and consequently allows coverage or capacity gains, with the use of directional antennas in ad hoc networks; *(2) da Conceição* and *Kon* [Conceição 2006] analyzed experimentally in IEEE 802.11b WLANs the impact on the application layer of interference, link range, mobility and coverage.

To the best of our knowledge, in spite of the intensive research activity upon IEEE 802.11 link analyses issues, there is room in the open literature for analytical

works that take into account the channel load, goodput, channel modelling, receiver structures and link analyses in an integrated way. Some of the earlier referenced papers have estimated the link budget, but they have not presented a systematic methodology to correlate the link analyzes with channel modeling, traffic load and goodput.

On other hand, based on the methodology proposed by Bianchi [Bianchi 2000], we have been developing a cross-layer theoretical model that allows assessing the goodput and delay of IEEE 802.11a WLANs operating under saturation traffic over uncorrelated [Hoefel 2005] and correlated fading channels [Hoefel 2006]. Therefore, in the present contribution we have extended our previous theoretical results by: *(1)* developing a MAC and PHY cross-layer model that allows to calculate the link budget and to estimate the cell coverage jointly with aspects regarding the system performance (channel load, goodput, and so on); *(2)* extending our previous results by developing and validating an analytical model to estimate the saturation goodput of IEEE 802.11b and 802.11g networks; *(3)* comparing, using a unified methodology, the system performance and cell range of IEEE 802.11a, 802.11b and 802.11g networks.

To accomplish our goals, this paper is organized as follows. Section 2 summarizes fundamental characteristics of the high rate direct sequence spread spectrum (HR/DSSS) complementary code keying (CCK) IEEE 802.11b PHY layer. Section 3 describes the IEEE 802.11a PHY layer. Section 4 describes the extended-rate PHY (ERP) layer IEEE 802.11g operating under request-to-send/clear-to-send (RTS/CTS) scheme. A methodology to calculate the link budget to 802.11 WLANs is developed in Section 5. Section 6 presents a comparative performance assessment of goodput and cell coverage of IEEE 802.11a, 802.11b and 802.11g WLANs over flat fading Rayleigh channels. Finally, our conclusions are drawn in Section 7.

In this contribution, we have assumed that the IEEE 802.11 networks are operating under the distributed coordination function (DCF) RTS/CTS scheme over flat fading temporally uncorrelated Rayleigh channels.

2. HR/DSSS CCK IEEE 802.11b PHY Layer Parameters

In this section we have summarized the parameters of the HDR/DSSS CCK IEEE 802.11b PHY layer, which operates at bit rate R_b=*5.5 Mbps* and R_b=*11 Mbps* [Gast 2005]. We also model the packet loss rate for a system where all the nodes implement a maximum ratio combining receiver (MRC) [Proakis 2000] with L spatially uncorrelated antennas over a temporally uncorrelated flat fading Rayleigh channel.

The 802.11b PHY layer has 14 channels in the 2.4 GHz band, each 5 MHz wide. Most of the networks are implemented using the nonoverlaping channels 1, 6 and 11. The RTS control frame has N_{rts}=*160 bits*. Both the CTS and acknowledge (ACK) control frames have N_{cts}= N_{ack} =*128 bits.* [Gast 2005]. The length of the medium access control (MAC) frames is given by

$$T_x(p_x) = T_{pp} + T_{ph} + \frac{N_x}{R_b}, \quad (1)$$

where x stands for the labels RTS, CTS and ACK (e.g. p_{rts} denotes the PHY mode used to transmit a RTS control frame). T_{pp} denotes the preamble duration and T_{ph} labels the PHY layer convergence procedure (PLCP) header.

The PHY layer protocol data unit (PDU) has a preamble, a PLCP header and the encapsulated MAC PDU (MPDU) [GAST 2005, p. 269]. It is assumed that the framing

is carried out using the short preamble with $N_{pp}=72$ *bits*. The PLCP header has $N_{ph}=48$ *bits*. The PLCP preamble is transmitted using differential binary phase-shift keying (DBPSK) at *1 Mbps*. The PLCP header is transmitted using differential quaternary phase-shift keying (DQPSK) at *2 Mbps*. Therefore, $T_{pp}=72\mu s$ and $T_{ph}=24\mu s$. The PLCP service data unit can be transmitted using *5.5* or *11 Mbps* complementary code keying (CCK). The chip rate (R_c) is set to *11 Mchips/s* for all bit rates.

The length of MAC data frames is given by

$$T_d(p_d) = T_{pp} + T_{ph} + \frac{8 \cdot \mathrm{N_{mh}} + 8 \cdot \mathrm{l_{pl}}}{\mathrm{R_b}}, \tag{2}$$

where p_d denotes the PHY mode used to transmit the data frame (i.e. p_d can be CCK at 5.5 Mbps or CCK at 11 Mbps) and l_{pl} denotes the payload length. The MAC data header (N_{mh}) has *32 bytes*, i.e. it consists of 24 bytes for the header, 4 bytes for the frame checking sequence [GAST 2005, p. 75] plus 4 bytes for the wireless equivalence privacy (WEP) scheme [GAST 2005, p. 123]. In the present paper, the control and data frames are transmitted using the same PHY mode (i.e. $p_{cts}= p_{rts}=p_{ack}= p_d$).

Assuming an MRC receiver with L antennas operating over an uncorrelated flat fading Rayleigh channel, then the average bit error rate (BER) for DBPSK can be estimated by [Proakis 2001, p. 827]

$$\mathrm{P_{dbpsk}} \approx \left(\frac{1}{2 \cdot \bar{\gamma}_b}\right)^L \binom{2L-1}{\mathrm{L}}, \tag{3}$$

where $\bar{\gamma}_b = \mathrm{E_b}/I_0$ is the signal-to-interference-plus-noise ratio (SINR) per bit, E_b is the energy per bit and I_0 is the one-side power spectral density modeled as additive white Gaussian noise (AWGN).

Assuming again an uncorrelated flat fading Rayleigh channel with spatial diversity L, the BER for DQPSK modulation can be estimated by [Proakis 2001, p. 831]

$$\mathrm{P_{dqpsk}} = \frac{1}{2} \cdot \left(1 - \frac{\mu}{\sqrt{2-\mu^2}} \cdot \sum_{k=0}^{L-1} \binom{2k}{k} \cdot \left(\frac{1-\mu^2}{4-2\mu^2}\right)\right), \tag{4}$$

where $\mu = \dfrac{\bar{\gamma}_b}{1+\bar{\gamma}_b}$. (5)

The SINR per bit is modeled as

$$\bar{\gamma}_b = \frac{P_r}{I_0 \cdot R_b} = G_p \frac{P_r}{I_0 \cdot R_c}, \tag{6}$$

where P_r is the received power and $G_p=R_c/R_b$ is the processing gain. In the case of *BDPSK* and *DQPSK* signaling schemes, the pseudo-noise (PN) code is the 11-chip long Barker code (i.e. $G_p=11$).

CCK is a variation of M-ary Biorthogonal (MBOK) modulation, which is composed of M unique nearly orthogonal codewords [Faiber 2001]. *M orthogonal* and *M biorthogonal* signaling schemes have similar performance when M and the SINR per symbol are large [Wozencraft 1965, p. 263]. Hence, assuming an uncorrelated flat fading Rayleigh channel with spatial diversity L and non-coherent square-law detected, the average BER can be estimated by [Proakis 2001, p. 834]

$$P_{cck} = \frac{2^{k-1}}{2^k - 1} \sum_{m=1}^{M-1} \frac{(-1)^{m+1} \binom{M-1}{m}}{(1 + m + m \cdot \bar{\gamma}_c)^L} \times \sum_{k=0}^{m(L-1)} \beta_{km} (L-1+K)! \left(\frac{1+\bar{\gamma}_c}{1+m+m\bar{\gamma}_c} \right)^k , \quad (7)$$

where $\bar{\gamma}_c$ is SINR per codeword. Since the chip rate is R_c=*11 Mchips/s* for both bit rates, then we have the following parameters: *(1) M=4*, G_p=*2* and $\bar{\gamma}_c = 2E_b / I_0$ for R_b=*5.5 Mbps; (2) M=8,* G_p=*1* and $\bar{\gamma}_c = E_b / I_0$ for R_b=*11 Mbps* [IEEE 802.11b 1999, p. 44-5]. β_{km} is a set of coefficients in the following expansion:

$$\left(\sum_{k=0}^{L-1} \frac{U_1^k}{k!} \right)^m = \sum_{k=0}^{m(L-1)} \beta_{km} U_1^k . \quad (8)$$

It is assumed that the BER is independent from bit to bit [Faiber 2001]. The PCLP header is always transmitted using DQPSK. Therefore, the probability that the RTS, CTS and ACK control frames are transmitted with success is given by

$$S_x = (1 - P_{dqpsk})^{N_{ph}} (1 - P_{cck})^{N_x} , \quad (9)$$

where *x* stands for the labels RTS, CTS or ACK. Correspondingly, the probability that a data frame with l_{pl} octets be transmitted with success is given by

$$S_d = (1 - P_{dqpsk})^{N_{ph}} (1 - P_{cck})^{8 \cdot (N_{mh} + l_{pl})} . \quad (10)$$

3. IEEE 802.11a PHY Layer

The IEEE 802.11a was designed for the 5 GHz Unlicensed National Infrastructure Band in the USA and it is based on Orthogonal Frequency Division Multiplexing (OFDM) using 52 subcarriers, of which 48 subcarriers carry actual data and 4 subcarriers are pilots used to implement coherent detection [IEEE 802.11a 1999]. The OFDM symbol interval, *tSymbol*, is set to 4μs. So, the channel symbol rate R_s is of *12 Msymbols/sec*.

Tab. 1 shows the OFDM PHY modes [IEEE 802.11a 1999]. *BpS* means Bytes per Symbol (e.g. the *PHY mode 1* carries 3 bytes per symbol, i.e. 6 Mbps* *tSymbol/8.0=3 BpS*). A description of the PHY parameters as well as the packet loss rate over flat fading Rayleigh channels over uncorrelated and correlated fading channels can be found in [Hoefel 2005] and [Hoefel 2006], respectively.

Tab. 1. The IEEE 802.11a and 2802.11g ERP-OFDM PHY modes.

Mode p	*Modulation*	*Code Rate R_c*	*Data Rate*	*BpS*
1	BPSK	1/2	6 Mbps	3
2	BPSK	3/4	9 Mbps	4.5
3	QPSK	1/2	12 Mbps	6
4	QPSK	3/4	18 Mbps	9

Mode p	*Modulation*	*Code Rate R_c*	*Data Rate*	*BpS*
5	16-QAM	1/2	24 Mbps	12
6	16-QAM	3/4	36 Mbps	18
7	64-QAM	2/3	48 Mbps	24
8	64-QAM	3/4	54 Mbps	27

The time period spent to transmit a MPDU with a payload of l_{pl} *octets* over the IEEE 802.11a using the *PHY mode* p_{mp} is given by (11). The length of RTS, CTS and ACK control frames are given by (12-13), respectively. The physical layer convergence procedure (PLCP) preamble duration, *tPCLPPreamble*, is equal to *12* μs and the PCLP

field duration, *tPCLP_SIG*, is equal to *4 μs*. The RTS and CTS have l_{rts}=*20 bytes* and l_{cts}=*14 bytes*, respectively. The ACK transmission time, assuming the *PHY mode* p_{akc} is given by (14), where its length is given by l_{ack}=*14 bytes* [Hoefel 2005].

$$T_{mp}(p_{mp}) = tPCLP\_\mathrm{Pre} + tPCLP\_SIG + \left\lceil \frac{l_{pl} + 34 + (16+6)/8}{BpS(p_{mp})} \right\rceil \cdot tS \quad (11)$$

$$T_{rts}(p_{rts}) = tPCLP\_\mathrm{Pre} + tPCLP\_SIG + \left\lceil \frac{l_{rts} + (16+6)/8}{BpS(p_{rts})} \right\rceil \cdot tS \quad (12)$$

$$T_{cts}(p_{cts}) = tPCLP\_\mathrm{Pre} + tPCLP\_SIG + \left\lceil \frac{l_{cts} + (16+6)/8}{BpS(p_{cts})} \right\rceil \cdot tS \quad (13)$$

$$T_{ack}(p_{ack}) = tPCLP\_\mathrm{Pre} + tPCLP\_SIG + \left\lceil \frac{l_{ack} + (16+6)/8}{BpS(p_{ack})} \right\rceil \cdot tS \quad (14)$$

4. IEEE 802.11g Extended Rate Physical Layer

This paper is focused on the major mode of the IEEE 802.11g, i.e. the Extended-Rate PHY layer Orthogonal Frequency Division Modulation (ERP-OFDM). Basically, it was carried out minor changes in the 802.11a PHY layer in order to adapt to the 2.4 GHz band and to allow coexistence with older networks that implement the 802.11b standard.

The ERP-OFDM 802.11g PHY layer uses the same modulation mode of IEEE 802.11a PHY layer, as shown in Tab. 1. However, the RTS and CTS control frames are transmitted using the CCK/DSSS modulation scheme. This approach allows that the 802.11b and 802.11g stations (STAS) can coexist in the same area, since 802.11b STAs can listen the control frames transmitted by 802.11g STAs and, consequently, set their network allocation vectors (NAVs). Therefore, as shown in Fig. 1, if the transmission of RTS and CTS are successful then the sender STA can transmit its MPDU without interruption of other 802.11b STAs in the same area. Notice that this reservation scheme would be impossible if the RTS and CTS frame were transmitted using OFDM, since the 802.11b STAs could not decode this signalling scheme. The duration of the RTS and CTS control frames can be calculated using (1). The ACK control frame is transmitted using OFDM and, therefore, its length can be calculated using (14).

Analytical expressions to calculate the frame success probability for OFDM access modes (see Tab. 1) can be found in [Hoefel 2005] for uncorrelated flat fading Rayleigh channel (the instantaneous received power changes from symbol-to-symbol) and in [Hoefel 2006] for correlated flat fading Rayleig channel (the instantaneous received power remains fixed at each atomic cycle).

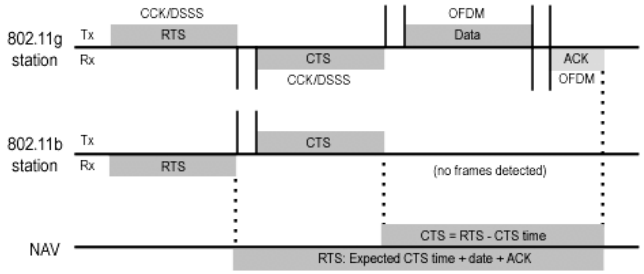

Figure 1. IEEE 802.11g operating under the RTS/CTS protection mechanism.

Hereafter, we use the following notation:

(1) S_{cts}, S_{rts} and S_{ack} denote, respectively, the probability that the RTS, CTS and ACK

control frames be transmitted with success;
(2) S_d denotes the probability that the transmission of a MPDU frame is successful;
(3) the window size at backoff stage i is labeled as $W_i = 2^i W$, where $i \in (0,m_{cw})$ is the backoff stage and W is the MAC contention window (CW) size parameter CW_{min};
(4) the maximum window size is denoted as $W_{mcw} = 2^{mcw} W - 1 = CW_{max} - 1$;
(5) n is the number of STAs in the system;
(6) SIFS is the short inter-frame spacing (IFS);
(7) DIFS is the distributed coordination function IFS.

We have shown in [Hoefel 2005] that for saturation traffic (i.e. all nodes always have a packet to transmit), the probability that a given station (STA) transmits in a randomly chosen slot time can be estimated by

$$\tau = \frac{b_{0,0}}{S \cdot (1-p)} = \frac{b_{0,0}}{S_{rts} \cdot S_{cts} \cdot S_d \cdot S_{ack} \cdot (1-p)}, \quad (15a)$$

$$b_{0,0} = \frac{2 \cdot (1-p) \cdot S \cdot [1+2 \cdot S \cdot (p-1)]}{1+2^{m_{cw}} W \cdot [1+(-1+p) \cdot S]^{m_{cw}} + (-1+p) \cdot S \cdot \{2+W+2^{m_{cw}} W \cdot [1+(-1+p) \cdot S]^{m_{cw}}\}}. \quad (15b)$$

The conditional probability that a transmitted PPDU have a collision given that a STA transmits in a slot time of length σ can be estimated given by

$$p = 1 - (1-\tau)^{n-1}. \quad (16)$$

The transmission probability and the conditional probability that the transmission collides p can be estimated by solving the nonlinear system given by (15) and (16).

The goodput in bits per second (bps) can be defined as the probability that an MPDU payload with l_{pl} *octets* be transmitted with success in the average cycle time $\overline{T}$:

$$G_{bps}(m) = \frac{8 \cdot l_{pl} \cdot P_s \cdot P_{tr} \cdot S_{rts} \cdot S_{cts} \cdot S_d \cdot S_{ack}}{\overline{T}}, \quad (17)$$

where the probability that there is no collision in the channel conditioned to the fact that at least one STA transmits is given by

$$P_s = \frac{n \cdot \tau \cdot (1-\tau)^{n-1}}{P_{tr}} = \frac{n \cdot \tau \cdot (1-\tau)^{n-1}}{1-(1-\tau)^n}, \quad (18)$$

and P_{tr} is the probability that there is at least one transmission occurs in the considered slot time of length σ.

The average cycle time is given by

$$\overline{T} = \overline{B}_s + \overline{B}_{f1} + \overline{B}_{f2} + \overline{B}_{f3} + B_{f4} + B_{f5} + \overline{I}. \quad (20)$$

The average busy time for a successful transmission is given by

$$\overline{B}_s = P_s \cdot P_{tr} \cdot S_{rts} \cdot S_{cts} \cdot S_d \cdot S_{ack} \cdot [DIFS + T_{rts}(p_{rts}) + a + SIFS + T_{cts}(p_{cts}) + a + SIFS + T_d(p_d) + a + SIFS + T_{ack}(p_{ack}) + a], \quad (21)$$

where a is the propagation delay, $T_{rts}(p_{rts})$ is the time necessary to transmit the RTS control frame when it is used the PHY mode p_{rts}. Correspondingly, $T_{cts}(p_{cts})$, $T_d(p_d)$ and $T_{ack}(p_{ack})$ denote the time necessary to transmit CTS, MPDU and ACK frames when it is used the PHY modes p_{cts}, p_d and p_{ack}, respectively. Expressions to calculate the length of RTS, CTS, MPDU and ACK frames can be found in earlier sections.

$\overline{B}_{f1}$ models the average amount of time in which the channel is busy due to collisions in the transmission of RTS control frames. $\overline{B}_{f1}$, $\overline{B}_{f2}$, $\overline{B}_{f3}$, $\overline{B}_{f4}$ and $\overline{B}_{f5}$

model the average time in which the channel is busy with unsuccessful transmissions of RTS, CTS, MPDU and ACK frames, respectively. The average time that a slot time with length σ is idle is given by (27).

$$\overline{B}_{f1} = P_{tr} \cdot (1 - P_s) \cdot [DIFS + T_{rts}(p_{rts}) + a] . \quad (22)$$

$$\overline{B}_{f2} = P_{tr} \cdot P_s \cdot (1 - S_{rts}) \ [DIFS + T_{rts}(p_{rts}) + a] . \quad (23)$$

$$\overline{B}_{f3} = P_{tr} \cdot P_s \cdot S_{rts} \cdot (1 - S_{cts}) \begin{bmatrix} DIFS + T_{rts}(p_{rts}) + a + \\ SIFS + T_{cts}(p_{cts}) + a \end{bmatrix}. \quad (24)$$

$$\overline{B}_{f4} = P_{tr} \cdot P_s \cdot S_{rts} \cdot S_{cts} \cdot (1 - S_{mp}) \ [DIFS + T_{rts}(p_{rts}) + a + SIFS + T_{cts}(p_{cts}) + a + SIFS + T_d(p_d) + a] . \quad (25)$$

$$\overline{B}_{f5} = P_{tr} \cdot P_s \cdot S_{rts} \cdot S_{cts} \cdot S_{mp} \cdot (1 - S_{ack}) [DIFS + T_{rts}(p_{rts}) + a + SIFS + T_{rcs}(p_{cts}) + a + SIFS + T_d(p_d) + a + SIFS + T_{ack}(p_{ack}) + a]. \quad (26)$$

$$\overline{I} = (1 - P_{tr}) \cdot \sigma \ . \quad (27)$$

5. Link Budget

The link budget is a balance sheet of power gains and losses. It takes into account the effects of transmission and reception resources, noise and interference sources, signal attenuation and fading. Tab. 2 shows a link budget for radio channel link access in IEEE 802.11 networks. The detailed explanation of each row entry is shown below Tab. 2.

Tab. 2. Access point to mobile stations link budget.

Line	Symbol	Link Budget	Default Value	Notes:
1	P_{tx}	Transmitter Power *(dBm)*		
2	L_{conc}	Connectors Loss *(dB)*		
3	L_{cable}	Cable Loss *(dB)*		
4	**P_{ir}**	**Power of the Intentional Radiator *(dBm)***		(#1-#2-#3)
5	G_{tx}	Transmitter Antenna Gain *(dBi)*		
6	**EIRP**	**Transmitter EIRP *(dBm)***		(#4+#5)
7	L_p	Path Loss *(dB)*		
8	X_σ	Shadowing Margin *(dB)*	8	
9	G_{rx}	Receiver Antenna Gain *(dBi)*	0	
10	**P_{rx}**	**Received Power *(dBm)***		(#6-#7-#8+#9)
11	R_b	Data Rate (dB-bit/s)		
12	**E_b**	**Energy per bit (dB-Joules)**		(#10-#11)
13	N_o	Noise Spectral Density *(dBm/Hz)*	-174	
14	W	System Bandwidth dB-Hz		
15	F	Noise Figure *(dB)*	5	
16	**N**	**Noise Power *(dBm)***		(#13+#14+#15)
17	M_I	Interference Margin *(dB)*	3	
18	**I**	**Interference-plus-noise power (dBm)**		(#16+17)
19	**$(SINR)_{rx}$**	**Received SINR *(dB)***		(#12-#18)
20	**$(SINR)_{est}$**	**Estimated E_b/N_o *(dB)***		

1. The transmitted power is set to attend the following constraints: *(a)* it must be less than the maximum transmitted power available (e.g. 15 dBm for Orinoco cards and 30 dBm for Proxim cards); *(b)* the maximum effective isotropic power must attend the maximum values allowed by the regulatory agencies (see item 4).
2. The typical loss in connectors is 0.25dB per connector.
3. The typical loss range is from 1dB/m to 0.1 dB/m. For instance, the loss for the following cables are: (a) 100 dB/100m for the RG 58; (b) for 12 dB/100m for the Heliax ½"; (c) 7 dB/100m for Heliax 7/8".
4. The power output of the intentional radiator refers to the power at the end of the last cable or connector before the antenna.
5. Typical antenna gains: *(a)* 0 dBi for ommidirectional antenna; *(b)* 2dBi for a simple integrated antenna; *(c)* 5 dBi for a simple external antenna.
6. The maximum EIRP is regulated by state agencies, such as Federal Communication Commission (FCC) in the USA and European Telecommunications Standards Institute (ETSI) in European Union. The FCC limits the EIRP as follows: *(a)* 30 dBm for 802.11b/g [Gast 2005, p.257]; *(b)* 22 dBm (channels 36-48) and 29 dBm (channels 52-64) for 802.11a [IEEE 802.11a 1999]. On the other hand, the ETSI limits the EIRP by 20 dBm for 802.11b/g [Gast 2005, p. 257]. The maximum EIRP set by the Brazilian Telecommunications Agency (ANATEL) is given by: (a) 26 dBm for the 2.4 GHz range; (b) 20 dBm for the bandwidth between 5.15 to 5.35 GHz. In this paper, we have assumed the typical values of 24 dBm for 802.11b and 802.11g and 20 dBm for 802.11a since the Wi-Fi products are traded worldwide [Gast 2005, p. 447]. The EIRP is given by (28). In this paper we have fixed the EIRP, then we must set the power delivery by the 802.11 card using (29).

$$EIRP = P_{tx} - L_{conc} - L_{cable} + G_{a,tx}. \tag{28}$$

$$P_{tx} = EIRP + L_{conc} + L_{cable} - G_{a,tx} \tag{29}$$

We have assumed a path loss model based on the breakpoint model. It has the free space loss distance exponent (*n=2*) for the first 10 meters and a distance exponent of *n=3.5* when the distance *d* increases above the breakpoint. Hence, the path loss can be written as

$$L_p(\mathrm{d}) = L_0 + \begin{cases} 20\log d, & 1 < \mathrm{d} \le 10\,\mathrm{m} \\ 20 + 20 + 35\log\dfrac{d}{10}, & \mathrm{d} > 10\,\mathrm{m} \end{cases}, \tag{30}$$

where L_0 is the free space path loss at reference distance of 1m:

$$L_0 = 40\log\frac{4\pi \cdot f}{c}, \tag{31}$$

where *f* is the frequency and *c* is velocity of light [Hashemi 1993].

7. The shadowing is modeled by a log-normal random variable with zero mean and standard deviation of *8 dB* [Clark 2002]. Therefore, the shadowing fading margin X_σ is set *8* dB.
8. The STAs use ommidirectional antennas (i.e. gain of 0 dBi).
9. The received power as a function of the distance *d* is given by

$$P_{rx,i}(\mathrm{d}) = EIRP - L(\mathrm{d}) - X_\sigma + G_{rx}. \tag{32}$$

10. The data rate depends upon the PHY layer (see Table 1).
11. The energy per bit in a linear scale is given by *P/R*, where *P* denotes the power and R_b the bit rate [Sklar 2001, p. 185]. So, the energy per bit in *dB-Joules* is given by

$$E_b = P_{rx} - R\,. \tag{33}$$

12. The one side noise spectral density N_0 models the additive white Gaussian noise (AWGN) at the receiver input. It is given by

$$N_0 = k \cdot T_0\,, \tag{34}$$

where the Boltzaman constant k is equals to *–198.60 dBm/K-Hz* and T_o is the effective noise temperature in degrees Kelvin (k). Assuming, T_0=*270* ^{0}*K* (24.31dB/K), then N_o = *-174 dBm/Hz.*

13. The bandwidth *W* depends on the PHY layer: (a) *W=20 MHz (73 dB-Hz)* for 802.11a; (b) W=*22 MHz (73.4 dB-Hz)* for 802.11b and 802.11g.
14. The noise figure *F* is defined by the ratio of the SINR at the input of a network to the SNR at the output at the network. It measures the noise introduced by the front-end amplifier at the receiver. We have assumed a typical value of *5 dB*.
15. The noise power in dBm at the detector input is given by

$$N = N_0 + W + F\,. \tag{35}$$

16. The interference margin counts for co-channel interference, non-linear intermodulation effects, etc. It is assumed a value of 3 dB [Clark 2002].
17. The total interference-plus-noise in *dBm* is given by

$$I = N_0 + W + F + M\,, \tag{36}$$

and, consequently, the interference-plus-noise spectral density in dB/Hz is given by

$$I_0 = N_0 + F + M\,. \tag{37}$$

18. The received SINR in linear scale is generically calculated by (38) [Sklar 2001, p. 185]. Therefore, the energy per bit to one side noise spectral density received at the detector input in dB is given by (39). The equation (39), using (32), can be rewritten as (40).

$$SINR = \frac{E_b}{I_0} = \frac{P_{rx}}{I_0}\left(\frac{1}{R_b}\right). \tag{38}$$

$$(SINR)_{rx} = P_{rx} - N_0 - F - M - R_b\,. \tag{39}$$

$$(SINR)_{rx} = EIRP - L(d) - X_\sigma + G_{rx} - N_0 - F - M - R_b\,. \tag{40}$$

19. The lower bound for the received SINR can be set by the following means: *(a)* analytically; *(b)* simulation; *(c)* field measures. In this paper, we have used the analytical framework developed in Sections 2 to 4.
20. Our objective is to estimate the cell range *d* given a system configuration and a performance target (that is determined by $SINR_{rx}$). Hence, from (40), we can determine the maximum path loss using (41). Finally, the maximum cell range *d* can be estimated using (30).

$$L(d) = EIRP + G_{rx} - (SINR)_{rx} + -X_\sigma - N_0 - F - M - R_b\,. \tag{41}$$

6. Performance Analyses of IEEE 802.11a, 802.11b and 802.11g WLANs

In this section we have compared simulation and analytical results for the goodput and present numerical results for the cell range of 802.11 WLANs.

The description of the IEEE 802.11 joint MAC and PHY layer simulator can be found in [Hoefel 2005].

Tab. 3 shows the IEEE 802.11 PHY layer parameters [Gast 2005]. The 802.11g WLAN is set up to operate in the ERP-OFDM mode, as defined in Section 4. We also

have assumed the following parameters: propagation time of $a=1\mu s$, payload length of $l_{pl}=1023$ *octets,* the channel is loaded with 10 STAs. The multipath radio environment is modeled as uncorrelated flat fading Rayleigh channel. The receiver implements a MRC technique with L receiving antennas, where the fading is uncorrelated at each antenna. The simulation results refer to a confidence interval of 98%.

Tab. 3. PHY layer parameters.

Parameters	802.11a	802.11b	802.11g
Slot time σ	9 µS	20 µS	20 µS
SIFS	16 µs	10 µS	10 µS (16 µS between data and ACK)
DIFS	34 µs	50 µs	50 µs
CW_{min}	16	31	32
CW_{max}	1023	1023	1023
Preamble Duration	20 µs	72µs	20 µs
PLCP header duration	4 µs	24µs	4 µs

We show in Fig. 2 analytical and simulation results for goodput as a function of SINR per bit for an 802.11a WLAN without (*L=1)* and with *(L=3)* spatial diversity. These results can also be found in [Hoefel 2005]. However, they are repeated here due to the following reasons: *(1)* we compare them with our original results on goodput of IEEE 802.11b and 802.11g networks (see Figs. 4 and 6); *(2)* we draw conclusions upon interrelations among goodput, SINR and cell range (see Fig. 3). In Fig. 2, we only show results for the PHY modes that optimise the system performance, i.e. PHY modes 3, 5, 7 and 8 for a system with *L=1* receiving antenna and PHY modes 3,5, 6, 7 and 8 for a system with *L=3* receiving antennas. Given an average SINR, the better performance of a given PHY mode in relation to other PHY modes depends upon a multitude of factors (e.g. type and cardinality of the modulation scheme; code rate of the convolutional code; channel modelling, etc.), as detailed in [Hoefel 2005].

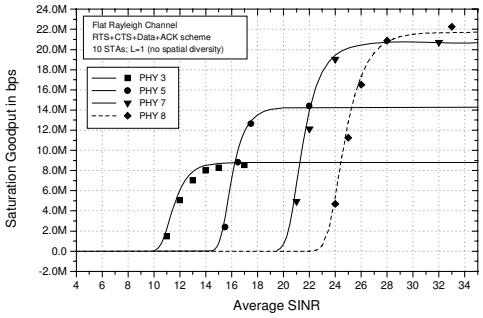

Figure 2a. No spatial diversity (L=1).

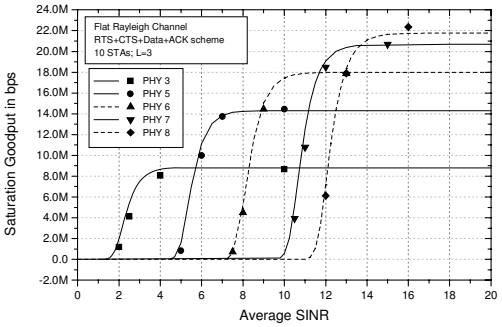

Figure 2b. Spatial diversity with 3 receiving antennas.

Figure 2. Comparison between analytical (straight lines) and simulation (marks) results for the saturation goodput in bps for all IEEE 802.11a PHY modes as a function of SINR per bit at detector input. Rayleigh flat fading.

We show in Fig. 3, using the same parameters employed at Fig.2, the cell coverage as a function of the goodput. The cell range is estimated using (41), where the values of $(SINR)_{rx}$, and their connections with the goodput, are obtained from Fig. 2. We can also observe the considerable gain in the cell range due to the spatial diversity.

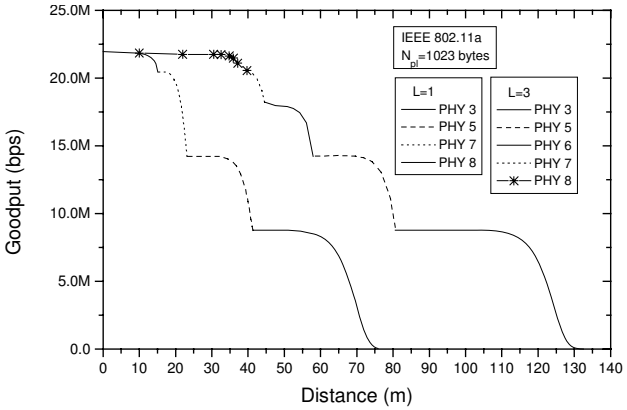

Figure 3. Cell coverage versus goodput for IEEE 802.11a. EIRP=-20 dBm. Channel 36 (fc=5.180 GHz). l_{pl}=1023 bytes.

We show in Fig. 4 results for goodput versus SINR per bit for the HR/DSSS CCK 802.11b WLAN without *(L=1)* and with spatial diversity *(L=3)*. First, we notice a good agreement between analytical (straight lines) and simulation (marks) results. Second, we can see that for a payload length of *1023 bytes*, the overhead consumes approximately *31%* and *45%* of the band for the gross bit rate of 5.5 and 11 Mbps, respectively. Notice that the greater gross bit rate is, then the greater the effects of DIFS and SIFS on the system performance are. Third, we can verify a tremendous gain due to spatial diversity (more than 30 dB). The HR/DDSS CCK PHY layer does not implement convolutional forward error correcting (FEC) coding and, therefore, just one bit error causes the corruption of the whole data packet. In this paper we have assumed an aggressive Rayleigh flat fading (non-line sight) and, consequently, the SINR must be high enough to avoid the packet corruption. For instance, an average BER of 13×10^{-5} is obtained with an average SINR of *40 dB* and *15.8 dB* for *L=1* and *L=3*, respectively (see Eq. 7). Therefore, the implementation of FEC coding explains the superior performance of the 802.11a PHY layer (see Fig. 2) in relation to HR/DSS CCK 802.11b PHY layer (see Fig. 4). We observe that for *L=1,* the 802.11a PHY layer operating with mode 3 needs around *15 dB* to reach the maximum goodput of approximately 8 Mbps (see Fig. 2a), while the *11 Mbps* 802.11b needs more than *20 dB* to reach the maximum goodput of *6 Mbps* (see Fig. 4). Finally, we have concluded that the implementation of optional IEEE 802.11b PHY layer that implements convolutional code (i.e. Packet Binary Convolutional Coding, PBCC, [Gast 2005, p. 274]) can be a solution to improve the IEEE 802.11b performance over uncorrelated flat fading Rayleigh channels. This is a topic for a future research.

Fig. 5 uses Eq. 17 (plotted in Fig. 4) and Eq. 41 to plot cell range for the HR/DSS CCK 802.11b PHY layer. Notice that the cell range is shorter in relation to the one shown in Fig. 3 for the 802.11a PHY layer. First, we notice that our results shown in Fig. 4 are in agreement with the ones shown in [Faiber 2000], where *Faiber and Goodman* analyzed the range of 802.11b WLANs considering only PHY layer issues. Therefore, our results are more complete since we have been carrying out a MAC and PHY cross-layer analyzes, where the MAC and PHY layer parameters, traffic load, channel modeling, receiver structures are taken into account using an integrated methodology. Second, we notice that some white papers claim a superior range of 802.11b in relation of 802.11a networks. This occurs because they have used the radio

sensibility (which is the minimum signal level for the receiver to acceptably decode the information) to calculate the link budget. However, the radio sensibility does not consider the effects of fading and packet length on the system performance. To include these factors it is necessary to define a short-term fading margin in the link budget. This fading margin is not constant since it depends upon the environment, packet length and so forth. In our methodology, the fading margin is implicitly included in the calculation of the goodput since the goodput depends on the payload length and SINR per bit (see equations 17 to 25).

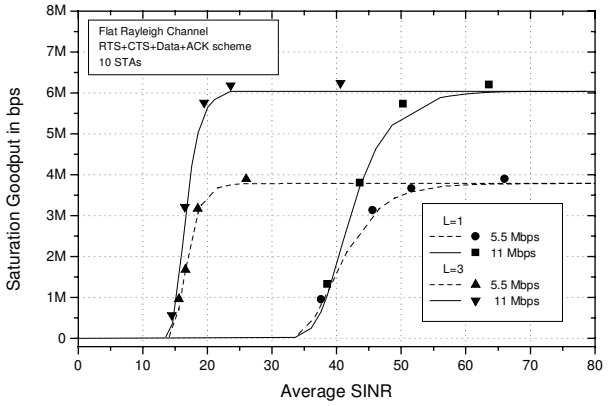

Figure 4. Comparison between analytical (straight lines) and simulation (marks) results for the saturation goodput in bps for 802.11b 5.5 and 11 Mbps modes versus SINR per bit at detector input. Rayleigh flat fading.

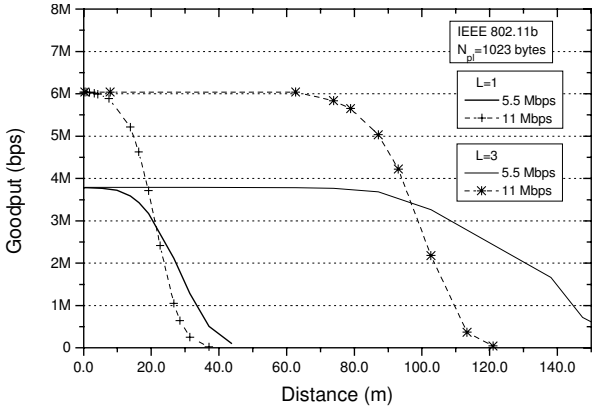

Figure 5. Cell coverage versus goodput for IEEE 802.11b. Rayleigh flat fading. EIRP=-26 dBm. Channel 1 (fc=2.412 GHz). N_{pl}=1023 bytes.

Fig. 6 shows results for goodput versus SINR per bit for the 802.11g ERP-OFDM WLAN without (*L=1)* and with *(L=3)* spatial diversity. Here, we assume that the RTS/CTS control frames are transmitted using CCK at 11 Mbps (see Fig.1). First, we notice again a good agreement between analytical (straight lines) and simulation (marks) results. Second, comparing Fig. 6 with Fig. 2 we can see that the 802.11a provides a superior performance. This occurs because in the 802.11g ERP-OFDM: *(1)* the RTS/CTS control frames are transmitted using the CCK modulation scheme. Notice that this modulation is more sensible to the fading due the lack of error control coding; *(2)* there is greater overhead due the DIFS and SIFS, as shown in Tab. 2. Fig. 6a shows that the better performance are obtained with PHY modes 7 and 8 with *L=1* receiving antenna, whereas Fig. 6b shows that a superior performance occurs with PHY modes 5, 7 and 8 for *L=3* receiving antennas. These results are different from the ones presented

at Fig. 2 because now the system is very sensible to errors that occur in the short length RTS and CTS control frames since they are transmitted without FEC coding. Third, comparing Fig. 6 with Fig. 4, we can see that 802.11g ERP/OFDM provides a superior performance in relation to the 802.11b PHY layer. This happens due to the use of improve modulation schemes and FEC coding (see Tab. 1) to transmit the MAC payload and ACK control frames (see Fig.1).

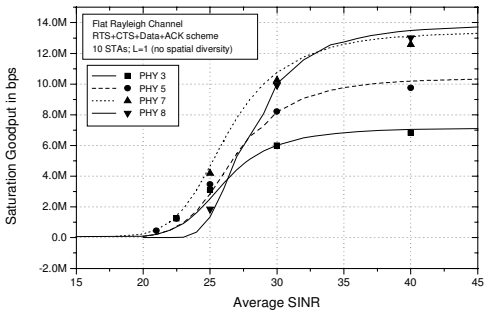

Figure 6a. No spatial diversity (L=1).

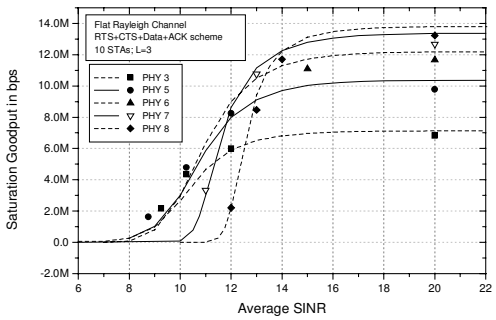

Figure 6b. Spatial diversity with 3 receiving antennas L=3.

Figure 6. Comparison between analytical (straight lines) and simulation (marks) results for the saturation goodput in bps for IEEE 802.11g PHY modes as a function of SINR per bit at detector input. Rayleigh flat fading.

Finally, Fig. 7 plots the cell range for 802.11g ERP-OFDM WLAN. Comparing with Fig. 4 we can immediately see that the 802.11g provides a superior bit rate and coverage in relation to 802.11b WLAN. We also plot in this figure the cell range for IEEE 802.11a and 802.11b with *L=1*. We can verify that 802.11a allows an improved cell range and net data rate. Basically, this happens due to beneficial effects of channel coding when the channel is modelled as temporally uncorrelated flat fading channel.

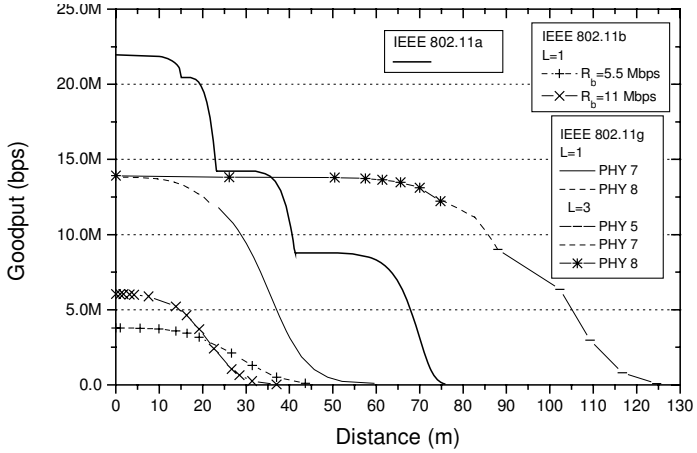

Figure 7. Cell coverage versus goodput for IEEE 802.11g. EIRP=-20 dBm. Channel 36 (fc=2.412 GHz). l_{pl}=1023 bytes.

7. Conclusions

We have developed and validated a first order analytical MAC and PHY cross-layer model that allows estimating the goodput and the cell range of IEEE 802.11a, HR/DSSS IEEE 802.11b, ERP/OFDM IEEE 802.11g WLANs networks. This model has been

driven by the following principles: *(1)* the pertinent physical properties are reflected in the model; *(2)* the simplified modeling is mathematically consistent and permissive to analyses; *(3)* it can be used as an auxiliary tool for complex simulation and mesasure campaigns, where it is possible to consider the multitude of features involved in analysis and design of 802.11 WLANs.

8. References

Bianchi, G. (2000) "Performance Analysis of the IEEE 802.11 Distributed Coordination Function," In: IEEE Journal on Selected Areas of Communication, v.18, no. 3, p. 535-547.

Clark, M. V., Leung, K. K., McNair, B., Kostic, Z. (2002) "Outdoor IEEE 802.11 Cellular Networks: Radio Link Performance," In: *Proc. of IEEE ICC*.

da Conceição, A. F. and Kon, F. (2006) "Developing Adaptive Applications over IEEE 802.11 Networks, " (in Portuguese) In: *24th Brazilian Symposium of Computer Networks*.

Faiber, M and Goodman, D. (2001) "Analysis of Interference Between IEEE 802.11 and Bluetooth Systems," In: *IEEE VTC 2001 Fall.*

Gast, M. S. (2005) "*802.11 Wireless Networks*". New York: O'Reilly.

Hashemi, H. (1993) "The indoor radio propagation channel", In: *Proceedings of IEE*, v. 81, n. 7, p. 943-968.

Hoefel, R. P. F. (2005) "A Joint MAC and Physical Layer Analytical Model for IEEE 802.11a Networks Operating Simultaneously under RTS/CTS Access Scheme," In: *23th Brazilian Symposium of Computer Networks*.

Hoefel, R. P. F. (2006) "A MAC and PHY Cross-layer Analytical Model for the Goodput and Delay of IEEE 802.11a Networks Operating with Basic Access and RTS/CTS Access Schemes", In: *24th Brazilian Symposium of Computer Networks*.

IEEE 802.11a (1999) *"Part 11: Wireless LAN Medium Access Control (MAC) and Physical Layer (PHY) Specification – Amendment 1: High-Speed Physical Layer in the 5 GHz band",* supplemented to IEEE 802.11 standard.

Intersil (1998). "Tutorial on Basic Link Budget Analyzes", http://www.intersil.com.

Kappes, M.; Krishnakumar, A.S.; Krishnan, P. (2004) "Estimating signal strength coverage for a wireless access point", In: *Global Telecommunications Conference 2004*.

Proakis, J. G. (2001) "*Digital Communications",* New York, 3th edition.

Ramela, I and de Rezende, J. F. (2006) "Avoiding primary interference with directional antennas in Ad Hoc networks" (in Portuguese), In: *24th Brazilian Symposium of Computer Networks*, Curitiba.

Skalar, B. (2001) *"Digital Communications"*, Upper Saddle River: Pearson Education, 3th edition.

Wozencraft J. M. and Jacobs, I. M. (1965) "*Principles of Communication Engineering"*, New York: Jonh Wiley & Sons.